Inorganic Chemistry

Article

pubs.acs.org/IC

Expanded Porous MOF-505 Analogue Exhibiting Large Hydrogen Storage Capacity and Selective Carbon Dioxide Adsorption

Baishu Zheng,*[†,‡] Ruirui Yun,[†] Junfeng Bai,*[†] Zhiyong Lu,[†] Liting Du,[†] and Yizhi Li[†]

[†]State Key Laboratory of Coordination Chemistry, School of Chemistry and Chemical Engineering, Nanjing University, Nanjing 210093, People's Republic of China

[‡]Key Laboratory of Theoretical Chemistry and Molecular Simulation of Ministry of Education, School of Chemistry and Chemical Engineering, Hunan University of Science and Technology, Xiangtan 411201, People's Republic of China

Supporting Information

ABSTRACT: An expanded 4,4-paddlewheel-connected porous MOF-505-type metal–organic framework (MOF), $[Cu_2(PDEB)(H_2O)_2]\cdot xS$ (NJU-Bai12; NJU-Bai represents the Nanjing University Bai group and S represents noncoordinated solvent molecules) has been designed from a nanosized rectangular diisophthalate linker containing alkyne groups 5,5′-(1,4-phenylenedi-2,1-ethynediyl)bis(1,3-benzenecarboxylic acid). This MOF material possesses permanent microporosity with the highest Brunauer–Emmett–Teller surface area of 3038 $m^2\cdot g^{-1}$ and the largest unsaturated total hydrogen storage capacity of 62.7 $mg\cdot g^{-1}$ at 77 K and 20 bar among reported MOF-505 analogues. Additionally, NJU-Bai12 also exhibits excellent carbon dioxide (CO_2) uptake capacity (23.83 and 19.85 $mmol\cdot g^{-1}$ at 20 bar for 273 and 298 K, respectively) and selective gas adsorption properties with CO_2/CH_4 selectivity of 5.0 and CO_2/N_2 selectivity of 24.6 at room temperature.

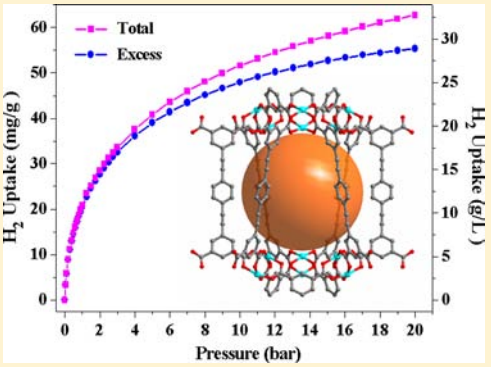

INTRODUCTION

Metal–organic frameworks (MOFs, also known as porous coordination polymers, PCPs) have been rapidly emerging as a new type of functional materials for catalysis,[1] magnetism,[2] luminescence,[3] drug delivery,[4] and sensing.[5] In particular, their large surface areas, adjustable pore sizes, and controllable pore surface properties make them good adsorbents in clean energy applications, such as hydrogen (H_2) storage,[6] methane (CH_4) storage,[7] and carbon dioxide (CO_2) capture.[8] In terms of capacity, MOFs currently hold the highest records in porous materials for H_2 uptake based on physical adsorption[9] and CH_4[7b] and CO_2 storage.[9b] To develop high-performance porous MOF materials for such applications, a number of factors such as the pore size and shape,[10] surface area and pore volume,[11] catenation,[12] open metal sites,[13] and engineering of gas–sorbent interactions by various strategies[14] have been extensively explored, and the results show that the maximum excess gas adsorption capacity of a MOF at high pressure is mainly controlled by its surface area and pore volume.[15] Thus, how to design MOFs with high porosity is one of the most important challenges for realization of high-capacity gas-storage MOF materials in the future. For a given framework topology, the best known strategy to increase its surface area is the use of elongated but geometrically equivalent organic linkers by virtue of the expanded pores.[16] For instance, recent studies show that replacing the phenyl spacers of organic linkers with triple-bond spacers can effectively boost the molecule-accessible gravimetric surface areas of MOFs and related high-porosity materials.[9a,17] Along this strategy, utilizing two hexacarboxylic acids prolonged by alkyne bonds, Hupp and co-workers[18] recently succeeded in obtaining two expanded *rht*-type MOF materials known as NU-109 and NU-110, which display the highest experimental Brunauer–Emmett–Teller (BET) surface areas of any porous materials reported to date (~7000 $m^2\cdot g^{-1}$).

The 4,4-paddlewhell-connected NbO-type MOF-505 series of porous MOFs have attracted tremendous attention in the past decade because catenation (interpenetration or interweaving of multiple frameworks) is difficult in such cage-based MOF networks and, most importantly, these types MOF materials exhibit excellent gas sorption properties because of their high surface area, tunable pore size, and open copper(II) sites suitable for gas adsorption.[7a,13a,16a,19] The use of this topology was pioneered by Chen et al.[13a] and has been significantly further explored by the Zhou, Schröder, Suh, and other groups.[19] We are interested in the construction of novel porous materials from highly symmetric multidentate carboxylate ligands.[20] Capitalizing on NbO topology, we recently obtained a microporous MOF-505-type MOF material exhibiting high surface area and excellent gas uptake[20b] from a rigid tetracarboxylate ligand with alkyne groups. To enlarge the pore volumes of materials for gas storage, herein we report the design and synthesize of a new expanded MOF-505 analogue, NJU-Bai12, assembled from a rectangular ligand nanosized by an acetylene moiety [5,5′-(1,4-phenylenedi-2,1-ethynediyl)bis-(1,3-benzenecarboxylic acid) (PDEB); see Scheme 1] and

Received: July 21, 2012
Published: March 4, 2013

   dx.doi.org/10.1021/ic301598n | *Inorg. Chem.* 2013, 52, 2823–2829

Scheme 1. Structure of the Ligand PDEB

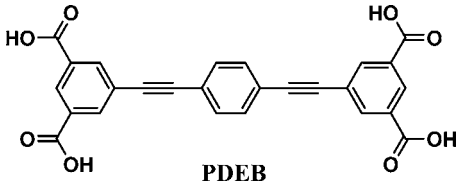

PDEB

paddlewheel $[Cu_2(COO)_4]$ secondary building units (SBUs). To our knowledge, NJU-Bai12 possesses the highest BET surface area of 3038 $m^2 \cdot g^{-1}$ and the largest unsaturated total H_2 storage capacity of 62.7 $mg \cdot g^{-1}$ at 77 K and 20 bar among reported MOF-505 analogues. Additionally, this MOF material demonstrates high and selective CO_2 adsorption at room temperature.

EXPERIMENTAL SECTION

General Information. All chemical reagents were obtained from commercial sources and, unless otherwise noted, were used as received without further purification. Elemental analyses (carbon, hydrogen, and nitrogen) were carried out on a Perkin-Elmer 240 analyzer. The IR spectra were obtained on a VECTOR TM 22 spectrometer with KBr pellets in the 4000−400 cm^{-1} region. ^1H NMR spectra were recorded on a Bruker DRX-500 spectrometer with tetramethylsilane as an internal reference. Thermogravimetric analyses (TGA) were performed under a N_2 atmosphere (100 mL/min) with a heating rate of 5 $°C \cdot min^{-1}$ using a 2960 SDT thermogravimetric analyzer. Powder X-ray diffraction (PXRD) data were collected on a Bruker D8 ADVANCE X-ray diffractometer using Cu Kα radiation (λ = 1.5418 Å) at room temperature with a routine power of 1600 W (40 kV and 40 mA) in a scan speed of 5°/min and a step size of 0.02 in 2θ. Simulation of the PXRD spectrum was carried out by the single-crystal data and diffraction-crystal module of the *Mercury* program available free of charge via the Internet at http://www. ccdc.cam.ac.uk/products/mercury/.

Synthesis of the Ligand 5,5′-(1,4-Phenylenedi-2,1-ethynediyl)bis-(1,3-benzenecarboxylic acid) (PDEB). This compound was synthesized according to the literature[21] and characterized by IR and ^1H NMR. Selected IR (KBr, cm^{-1}): 3420 (br, s), 1701 (s), 1594 (m), 1510 (m), 1442 (m), 1402 (m), 1335 (m), 1271 (s), 1245 (m), 1176 (m), 1108 (m), 1020 (m), 912 (m), 835 (m), 756 (m), 670 (m), 650 (m), 543 (m). ^1H NMR (DMSO-d_6, δ ppm): 13.53 (br peak, 4H, COO*H*), 8.46 (s, 2H, Ar*H*), 8.27 (s, 4H, Ar*H*), 7.71 (s, 4H, Ar*H*). Mp: >230 °C.

Synthesis of NJU-Bai12, $[Cu_2(PDEB)(H_2O)_2]\cdot xS$ (S = Solvent Guest Molecule). PDEB (11.33 mg, 0.025 mmol) and $CuCl_2 \cdot 2H_2O$ (17 mg, 0.1 mmol) in 2 mL of *N*,*N*-dimethylformamide (DMF) with 0.1 mL of water and 50 μL of HBF_4 were stirred for a few minutes in air, and the clear solution was transferred into a Teflon-lined stainless steel autoclave (20 mL). The autoclave was sealed and heated to 65 °C for 3 days and then cooled to room temperature at a rate 5 $°C \cdot h^{-1}$. Pale-green block crystals of NJU-Bai12 were obtained and then filtered and washed by DMF to yield 11.2 mg (yield: 73% based on the ligand). The crystals of NJU-Bai12 are stable for common organic solvents except for water; they become opaque after exposure to air for several minutes. Satisfactory microanalysis cannot be obtained because the extent of solvent molecules in the cavity may vary from exposure of the sample to air. Selected IR (KBr, cm^{-1}): 3412 (br, s), 1667 (vs), 1551 (s), 1516 (m), 1406 (s), 1362 (m), 1280 (m), 1242 (m), 1106 (m), 826 (m), 760 (w), 720 (w), 600 (w).

X-ray Crystallography. Single-crystal X-ray diffraction data of NJU-Bai12 were measured on a Bruker Smart Apex CCD diffractometer at 293 K using graphite-monochromated Mo Kα radiation (λ = 0.71073 Å). Crystals were sealed in capillaries containing a small amount of mother liquor to prevent desolvation during data collection. Data reduction was made with the Bruker *SAINT* program. The structure was solved by direct methods and refined with full-matrix least squares on F^2 with anisotropic displacement using the *SHELXTL* software package.[22] Non-hydrogen atoms were refined with anisotropic displacement parameters during the final cycles. Hydrogen atoms were placed in calculated positions with isotropic displacement parameters set to $1.2U_{eq}$ of the attached atom. In NJU-Bai12, free solvent molecules were highly disordered, and attempts to locate and refine the solvent peaks were unsuccessful. The diffused electron densities resulting from these residual solvent molecules were removed from the data set using the *SQUEEZE* routine of *PLATON*[23] and refined further using the data generated. The contents of the solvent region are not represented in the unit cell contents in the crystal data. Details of the crystal parameters, data collection, and refinements for NJU-Bai12 are summarized in Table S1 in the Supporting Information (SI).

Crystallographic data for NJU-Bai12: $C_{13}H_7CuO_5$, fw = 306.73, trigonal, $R\bar{3}m$, $a = b$ = 18.8306(6) Å, c = 52.557(3) Å, $\alpha = \beta = 120°$, $\gamma = 90°$, V = 16517.5(14) $Å^3$, Z = 18, T = 291(2) K, μ = 0.599 mm^{-1}, 30506 reflections were collected (3967 were unique) for $1.96° < \theta < 26.00°$, R(int) = 0.0548, R1 = 0.0367, wR2 = 0.0835 [$I > 2\sigma(I)$], R1 = 0.0570, wR2 = 0.0892 (all data), GOF = 1.027. CCDC 884077.

Low-Pressure Gas Sorption Measurements. Gas sorption isotherm measurements were performed on an ASAP 2020 surface area and pore-size analyzer. An as-isolated sample of NJU-Bai12 was soaked in anhydrous acetone for 3 days to remove the noncoordinated solvent molecules. During the exchange, acetone was refreshed six times. After removal of acetone by decanting, the wet acetone-exchanged sample was activated by drying under a dynamic vacuum at room temperature overnight to obtain activated NJU-Bai12 (NJU-Bai12-ac). Before measurement, the NJU-Bai12-ac sample was dried again by using the "degas" function of the surface area analyzer for 20 h at 110 °C. During this time, the pale-green sample changed to a purple-blue color indicative of desolvation of the open copper(II) sites; a similar color change upon activation was observed for other frameworks that were constructed from copper(II) paddlewheel clusters.[20d] UHP-grade (99.999%) N_2, Ar, H_2, CO_2, and CH_4 were used for all measurements. The temperatures were maintained at 77 (liquid-nitrogen bath), 87 (liquid-argon bath), 273, and 298 K, respectively. For all isotherms, warm and cold free-space correction measurements were performed using ultrahigh-purity helium gas (UHP grade 5.0, 99.999% purity). Part of the N_2 sorption isotherm at 77 K in the P/P_0 range of 0.005−0.01 was fitted to the BET equation to estimate the BET surface area, and Langmuir surface area calculation was performed using all data points. The pore-size distribution (PSD) was obtained from the DFT model in the Micromeritics ASAP 2020 software package (assuming cylinder pore geometry) based on the N_2 sorption isotherm.

High-Pressure Gravimetric Gas Sorption Measurements. High-pressure excess adsorption of H_2 (77 K), CO_2, CH_4, and N_2 (273 and 298 K) were measured using an IGA-003 gravimetric adsorption instrument (Hiden Isochema, Warrington, U.K.) over a pressure range of 0−20 bar. Prior to sorption measurements, ∼120 mg acetone-exchanged wet samples were loaded into the sample basket within the adsorption instrument and then degassed under high vacuum at 110 °C for 20 h to obtain ∼70 mg fully desolvated materials. At each pressure, the sample mass was monitored until equilibrium was reached (within 25 min). The total gas uptake was calculated by $N_{total} = N_{excess} + \rho_{bulk}V_{pore}$, where ρ_{bulk} equals the density of compressed gases at the measured temperature and V_{pore} was obtained from the N_2 isotherm at 77 K.[24]

Estimation of the Isosteric Heats of Gas Adsorption. A Virial-type[25] expression comprising the temperature-independent parameters a_i and b_i was employed to calculate the enthalpies of adsorption for H_2 (at 77 and 87 K), CO_2, CH_4, and N_2 (at 273 and 298 K). In each case, the data were fitted using the equation

$$\ln P = \ln N + 1/T \sum_{i=0}^{m} a_i N^i + \sum_{j=0}^{n} b_j N^j \quad (1)$$

Here, P is the pressure expressed in Torr, N is the amount adsorbed in $mmol \cdot g^{-1}$, T is the temperature in K, a_i and b_i are Virial coefficients, and m and n represent the number of coefficients required to

dx.doi.org/10.1021/ic301598n | *Inorg. Chem.* 2013, 52, 2823−2829

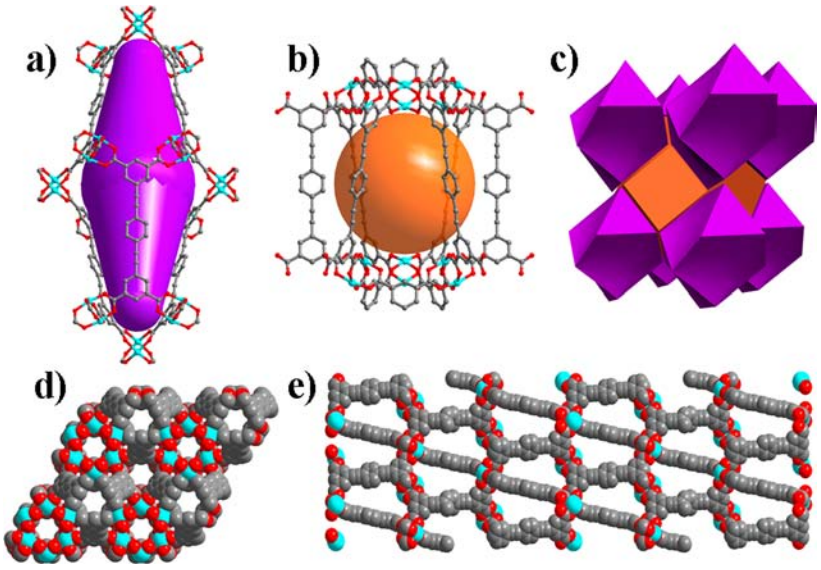

Figure 1. (a and b) Shuttle-shaped and spherical cage. (c) Natural tiling for NJU-Bai12 and (d and e) atomic packing of **1** viewed through the [0 0 −1] and [1 0 0] directions. Color code: Cu, green; C, gray; O, red. Water molecules and hydrogen atoms are omitted for clarity.

adequately describe the isotherms (m and n were gradually increased until the contribution of extra added a and b coefficients was deemed to be statistically insignificant toward the overall fit and the average value of the squared deviations from the experimental values was minimized). The values of the virial coefficients a_0–a_m were then used to calculate the coverage-dependent isosteric heat of adsorption (Q_{st}) using the following expression (R represents the universal gas constant):

$$Q_{st} = -R \sum_{i=0}^{m} a_i N^i \qquad (2)$$

RESULTS AND DISCUSSION

Single-Crystal X-ray Structure and Structural Stability of NJU-Bai12. A larger quantity of block-shaped pale-green crystals of MOF material NJU-Bai12 can be readily prepared by a solvothermal reaction of $CuCl_2{\cdot}2H_2O$ with PDEB in DMF containing a small amount of H_2O and HBF_4 at 65 °C for 3 days. Single-crystal X-ray crystallographic analysis revealed that NJU-Bai12, which is formulated as $[Cu_2(PDEB)(H_2O)_2]{\cdot}x$S (S = solvent guest molecule), crystallizes in the trigonal space group $R\bar{3}m$ with $a = b = 18.8306(6)$ Å and $c = 52.557(3)$ Å. As expected, in the structure of NJU-Bai12, the copper(II) ions form a paddlewheel-type $[Cu_2(COO)_4]$ cluster as a four-connected square-planar SBU, which is bridged by the four-connected rectangular organic building block PDEB to give rise to an expanded 3D 4,4-connected NbO-type structure, the same topology as that of the prototype framework, MOF-505 (Figure 1). Each copper(II) ion shows square-pyramidal geometry, with four oxygen atoms from four different PDEB units and a water molecule coordinated at the axial position of the paddlewheel unit.

A careful examination of the crystal structure reveals that there are two types of cages in the framework (Figures 1 and S1 in the SI). The first type is a shuttle-shaped cage with an inner-sphere diameter of ca 1.1 nm, in which 12 copper(II) paddlewheel SBUs occupied the vertices and 6 PDEBs occupied the faces (Figure 1a). The second type, a spherical-like pore of about 1.6 nm diameter, is surrounded by six PDEB and six copper(II) paddlewheel SBUs (Figure 1b). Both cages are arranged in an alternating fashion along to the c axis in a 1:1 ratio to form a cage-stacked 3D framework (Figure 1d). Because of the long organic linker, compared with the prototype MOF-505, a huger void space is created in NJU-Bai12. The void volume of NJU-Bai12 calculated by *PLATON*[23] is up to 74.3% of the unit cell volume without any guest molecules, and it increases to 78.2% (12922.3 Å^3 out of 16517.5 Å^3 per unit cell volume) upon removal of the coordinated water molecules with a low calculated density of only 0.522 g·cm^{-3}, highlighting the extremely porous nature of the framework.

The bulk identity and thermal stability of NJU-Bai12 were investigated by PXRD measurements and TGA. The TGA curve shows that the as-synthesized NJU-Bai12 lost ∼59% weight because of the DMF and H_2O guest solvent molecules filled in the pores, and the framework can be thermally stable up to 300 °C (Figure S2 in the SI). To obtain the fully desolvated framework (NJU-Bai12-ac), the as-synthesized NJU-Bai12 was repeatedly immersed in anhydrous acetone, and the guest solvent molecules can be exchanged with acetone to produce the acetone-exchanged sample, which was characterized by IR (see Figure S3 in the SI). The acetone-exchanged sample was then evacuated under high vacuum at 110 °C for 20 h, and a color change from pale green to deep purple-blue was observed, typical for copper(II) paddlewheel frameworks in which open copper(II) sites are generated.[26] NJU-Bai12-ac shows a similar weight loss curve (Figure S2 in the SI), which indicated the good stability of the framework. The robustness of the framework for NJU-Bai12 has been further examined by PXRD experiments, as shown in Figure 2; the similarity of the simulated PXRD pattern from single-crystal data to that for both as-synthesized and activated samples demonstrates that the single crystal is representative of the pure bulk sample, and the framework is robust and its crystallinity can be retained after removal of guest molecules.

Porosity of NJU-Bai12-ac. To investigate the permanent porosity of NJU-Bai12-ac, we performed low-pressure N_2 adsorption measurements at 77 K (Figure 3). The N_2 sorption at 77 K for NJU-Bai12-ac exhibited a reversible type I isotherm, a characteristic of microporous materials, which is coincidental

dx.doi.org/10.1021/ic301598n | *Inorg. Chem.* 2013, 52, 2823−2829

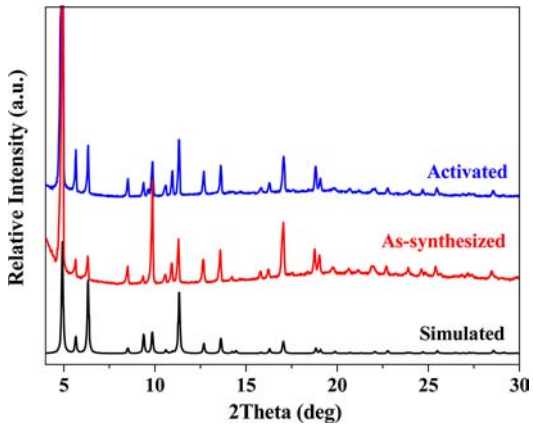

Figure 2. PXRD patterns of MOF material: A simulated PXRD pattern from the single-crystal structure, as-synthesized and activated for NJU-Bai12, respectively.

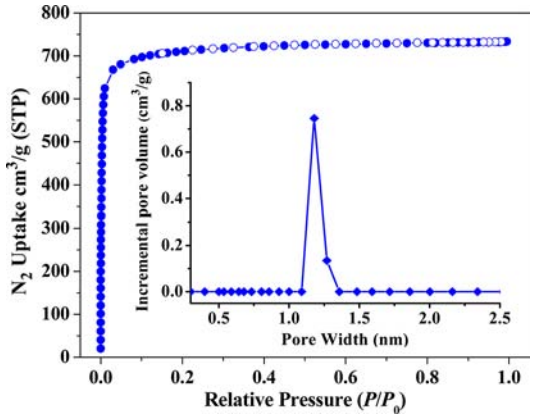

Figure 3. N_2 sorption isotherm at 77 K (filled circles, adsorption; empty circles, desorption) and PSD of NJU-Bai12-ac.

with the crystal structure. Significantly, NJU-Bai12-ac can take up a large amount of N_2 at 77 K (~750 $cm^3 \cdot g^{-1}$ at 1 bar), featuring an apparent BET surface area of 3038 $m^2 \cdot g^{-1}$ and a Langmuir surface area of 3208 $m^2 \cdot g^{-1}$. Notably, the experimental surface area of NJU-Bai12-ac is fairly comparable to the Connolly surface area estimated from the crystal structure (~3600 $m^2 \cdot g^{-1}$ using a probe of 3.68 Å diameter) using *Materials Studio* 5.5.[27] To the best of our knowledge, these values are smaller than those reported for NU-100 (~6143 $m^2 \cdot g^{-1}$),[9a] MOF-210 (~6240 $m^2 \cdot g^{-1}$),[9b] and NU-110 (~7140 $m^2 \cdot g^{-1}$)[18] but still represent the highest surface area reported to date for 4,4-connected NbO-type MOFs based on paddlewheel clusters[7a,13a,16a,19,20b] (Table 1). On the basis of the DFT model in the Micromeritics ASAP 2020 software package (assuming split pore geometry), NJU-Bai12-ac has a narrow PSD of around 1.18−1.27 nm (inset of Figure 3), which is consistent with the parameters of the cages in the crystal structure. The total pore volume of NJU-Bai12-ac calculated from the maximum amount of N_2 adsorbed at 77 K is 1.135 $cm^3 \cdot g^{-1}$.

H_2 Storage Property. Because of the high efficiency and zero-emissions operation, H_2 is considered as a compelling alternative to gasoline in many respects, and the development of an effective on-board H_2 storage system is one of the key technologies needed for practical applications.[28] In 2011, the U.S. Department of Energy (DOE) reset the gravimetric and volumetric storage targets for on-board H_2 storage for 2017 (5.5 wt %, 40 $g \cdot L^{-1}$).[29] Although none of the candidate materials developed so far has satisfied the DOE target yet, MOFs with large surface area have been regarded as one of the most promising H_2 storage materials and numerous MOFs with excellent H_2 storage capacity have been reported. Currently, the highest excess H_2 storage capacity reported so far for MOFs is 99.5 $mg \cdot g^{-1}$ at 56 bar and 77 K in NU-100,[9a] and the highest total H_2 storage capacity reported is 176 $mg \cdot g^{-1}$ (excess 86 $mg \cdot g^{-1}$) in MOF-210[9b] at 77 K and 80 bar. These values are symbolic of the tremendous advancement in research on MOFs as H_2 storage materials. For high H_2 uptake, the high surface area of the frameworks is believed to be the single factor of utmost importance. In addition, the pore size/geometry and presence of strongly interacting functional groups, such as exposed metal sites in high site density, also play important roles in high H_2 uptake.[25,30]

Table 1. Ligand Size, Porosity, and H_2 Storage Capacity of Some Representative NbO-Type MOFs

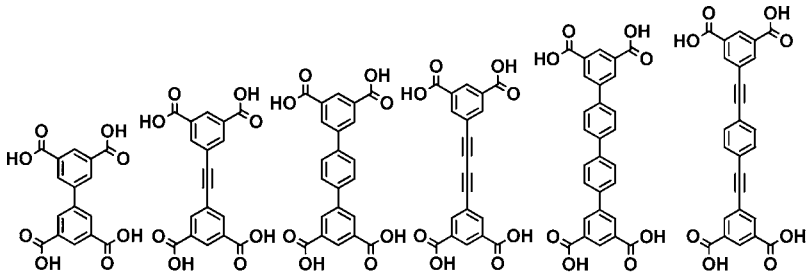

BPTC in **MOF-505** EBTC in **PCN-16** TPTA in **NOTT-101** BDI in **PCN-46** QPTA in **NOTT-102** PDEB in **NJU-Bai12**

MOF	ligand size [nm][a]	BET area [$m^2 \cdot g^{-1}$]	V_{pore} [$cm^3 \cdot g^{-1}$][b]	H_2 uptake at 77 K [$mg \cdot g^{-1}$][c]	Q_{st} at zero coverage [$kJ \cdot mol^{-1}$]
MOF-505	0.709	1670	0.680	25.9/40.2	6.3
PCN-16	0.959	2273	0.960	26.0/56.3	NA
NOTT-101	1.138	2247	0.886	25.2/60.6	<5.5
PCN-46	1.209	2500	1.012	19.5/61.5	7.2
NOTT-102	1.564	2932	1.138	22.4/60.7	<5.5
NJU-Bai12-ac	1.857	3038	1.135	19.1/62.7	6.8

[a]The ligand size is defined as the distance between the top carbon atoms of the terminal benzene rings. [b]Calculated from N_2 isotherms at 77 K. [c]Total uptake at 1 and 20 bar, respectively. NA = not available.

dx.doi.org/10.1021/ic301598n | *Inorg. Chem.* 2013, 52, 2823−2829

The high porosity and stable framework with open copper(II) sites suggest NJU-Bai12-ac as a promising candidate for H_2 gas storage. Low-pressure H_2 sorption isotherms were collected at 77 K, and as shown in Figure 4, NJU-Bai12-ac can

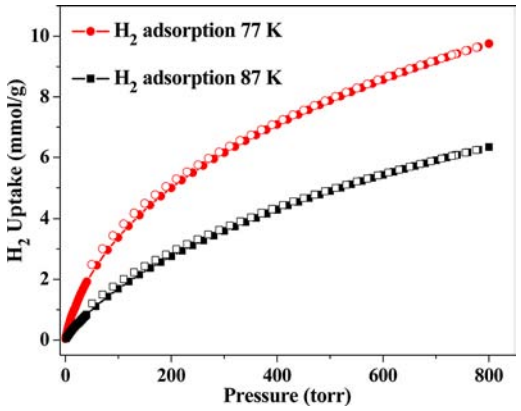

Figure 4. Low-pressure H_2 isotherms collected under 77 and 87 K for NJU-Bai12-ac.

reversibly adsorb 19.1 mg·g^{-1} of H_2 at 77 K and 1 atm, which is lower than the corresponding values of MOF-505 and other isostructural MOFs[13a,16a,19,20b] (Table 1) probably due to the larger pore size. To estimate the coverage-dependent H_2 adsorption enthalpies (Q_{st}), H_2 adsorption isotherms were also measured at 87 K, which adsorbs 12.3 mg·g^{-1} H_2 gas (Figure 4). On the basis of the Virial method,[25] the H_2 isosteric adsorption enthalpy of NJU-Bai12-ac reaches 6.8 kJ·mol^{-1} (Figure 5) at zero coverage and steadily decreased to 5.2

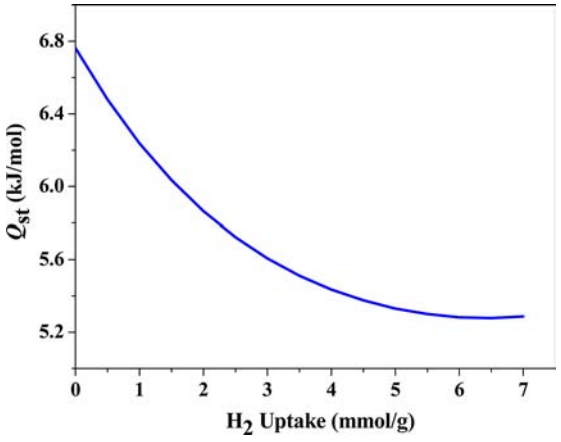

Figure 5. H_2 isosteric adsorption enthalpies for NJU-Bai12-ac.

kJ·mol^{-1} at medium loading. Interestingly, despite the larger pore size in NJU-Bai12-ac, this Q_{st} value is comparable to that of PCN-46 (~7.2 kJ·mol^{-1}) and fairly higher than the values of NOTT-101 and NOTT-102 (<5.5 kJ·mol^{-1}).[19f] A literature survey shows that such a phenomenon also exists in two isostructural rht-type MOFs:[31] NOTT-119 with alkyne groups possesses larger pores but exhibits higher Q_{st} (7.3 kJ·mol^{-1}) than that of NOTT-116 based on phenyl rings (6.7 kJ·mol^{-1}). Zhou and co-workers[19h] attribute such enhancenments of the H_2 adsorption enthalpy in MOFs with alkyne moieties to the stronger interaction between H_2 molecules and the delocalized π electrons in the alkyne units than that for the phenyl rings. In addition, a similar strong interaction between acetylene and a NbO-type MOF PCN-16 containing an alkyne unit was also discovered by us,[20b] in which the high acetylene affinity toward to the framework was partially attributed to $\pi-\pi$ interaction.

Because the H_2 adsorption isotherm is not saturated at 77 K and 1 atm, high-pressure H_2 adsorption was performed using a gravimetric measurement method as well to evaluate its H_2 adsorption performance. The excess H_2 uptake of NJU-Bai12-ac reaches up to 55.3 mg·g^{-1} at 20 bar and 77 K (Figure 6). It is

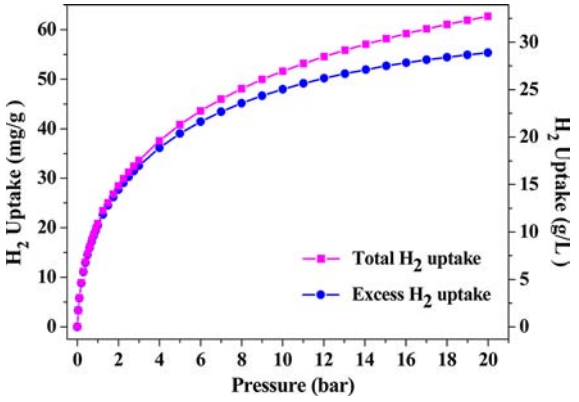

Figure 6. High-pressure gravimetric and volumetric H_2 uptake in NJU-Bai12-ac at 77 K (solid symbols, adsorption; open symbols, desorption).

worth noting that this storage capacity is far from saturated, which means that its uptake can be further maximized at a higher pressure range (restricted by the maximum pressure of the instrument, the H_2 sorption isotherm was recorded only from 0 to 20 bar in this work). Taking into consideration the gaseous H_2 compressed within the framework void, the total gravimetric H_2 uptake capacity can reach as high as 62.7 mg·g^{-1} at 20 bar and 77 K, which represents the highest values for the total H_2 adsorption on NbO-type MOF-505 series MOFs (Table 1) at the same conditions. This observation further verifies the thoerotical opinions that give the same MOF structural type: the longer the ligand, the higher the specific surface area and, accordingly, the higher the gravimetric H_2 uptake would be. Calculated from the crystal density of the activated form, NJU-Bai12-ac has an excess and total volumetric H_2 uptake of 28.9 and 32.7 g·L^{-1} at 20 bar, respectively.

Selective CO_2 Adsorption. The selective capture and sequestration of CO_2 has been considered to be an effective way of controlling greenhouse gas emissions. Most of the capture processes in large-scale operation nowadays are based on amine-based wet scrubbing systems, which have high energy and resource consumption.[32] Thus, great efforts have been dedicated to developing versatile CO_2 capture materials, and a number of porous solids such as zeolites, mesoporous silicas, hydrotalcites, and polymer-based adsorbents have been intensively tested.[33] More recently, it was demonstrated that MOFs exhibit charming properties with respect to CO_2 storage and separation.[8c,34] Large CO_2 adsorption capacities were reported for this young, rapidly growing class of porous materials.[9a,b,35] In particular, their exceptionally high surface areas and large overall pore volumes, uniform but adjustable pore sizes, and chemically tunable functional pores can be carefully designed for CO_2 capture and sequestration applications.[36]

The high surface area and large pore volume of NJU-Bai12 prompt us to examine its CO_2 adsorption behavior. To explore

dx.doi.org/10.1021/ic301598n | Inorg. Chem. 2013, 52, 2823−2829

the potential of NJU-Bai12-ac as CO_2 storage/separation materials, high-pressure CO_2, CH_4, and N_2 gravimetric sorption measurements have also been carried out at 298 and 273 K in the range of 0−20 bar. As shown in Figure 7, all isotherms

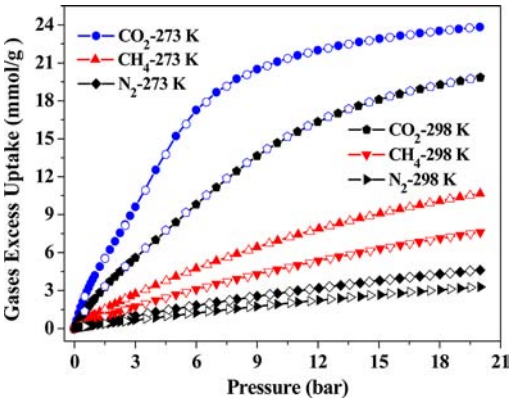

Figure 7. High-pressure gravimetric excess CO_2, CH_4, and N_2 uptake in NJU-Bai12-ac at 298 and 273 K, respectively (solid symbols, adsorption; open symbols, desorption).

show type I behavior as expected for materials with micropores. Similar to most of the other sorbents, CO_2 is the most strongly adsorbed in NJU-Bai12-ac and CH_4 shows stronger adsorption than N_2. This sorption behavior can be attributed to the fact that the higher quardrupole moment and polarizablility of CO_2 molecules may induce better interaction with the open copper(II) sites of the framework,[37] which can be further confirmed by Q_{st} values at zero coverage calculated from adsorption at 298 and 273 K through the Virial method, with values of 23.5, 15.7, and 14.1 kJ·mol^{-1} for CO_2, CH_4, and N_2 adsorption, respectively (Figure S4 in the SI). Most significantly, at 20 bar, high unsaturation excess CO_2 uptake values of 23.83 and 19.85 mmol·g^{-1} are observed at 273 and 298 K, respectively. This CO_2 storage capacity is comparable to that of NU-100[9a] (∼21.6 mmol·g^{-1}) and greater than that of most other high-surface-area MOFs reported such as MOF-210 (∼16 mmol·g^{-1}), MOF-200 (∼14.8 mmol·g^{-1}),[9b] and MOF-5 (∼19 mmol·g^{-1})[35a] at 20 bar and 298 K. Additionally, it is noted that, even though numerous high-surface-area MOFs have been reported, few exhibit a high CO_2 uptake of more than 19 mmol·g^{-1} under the same conditions.[8] Furthermore, a container filled with NJU-Bai12-ac can store about 12 times the amount of CO_2 in an empty container at 20 bar and 298 K based on the total capacity (this value increases up to 13 times at 273 K), which further suggests that NJU-Bai12-ac is a good CO_2 adsorbent.

In sharp contrast to CO_2, NJU-Bai12-ac can only absorb limited amounts of CH_4 (∼10.66 and 7.61 mmol·g^{-1}, 20 bar) and N_2 (∼4.62 and 3.29 mmol·g^{-1}, 20 bar) at 273 and 298 K, respectively, indicating that the guest-evacuated NJU-Bai12-ac has the ability to selectively adsorb CO_2 over CH_4 and N_2. The CO_2/CH_4 and CO_2/N_2 adsorption selectivities calculated from the slopes of the isotherms[38] reach up to 5.7 and 29.4 at 273 K, respectively (Figure S5 in the SI). With an increase in the temperature at 298 K, these values still reach 5.0 and 24.6, much higher than the corresponding values of MOF-177 (4.4 and 17.5)[39] and most other MOF materials (mainly in the ranges of 3−10 and 10−50 for CO_2/CH_4 and CO_2/N_2 selectivities at room temperature, respectively).[8c]

CONCLUSION

In summary, by using a nanosized rectangular diisophthalate linker prolonged by C≡C bonds (PDEB) as the linker and a copper(II) paddlewheel as the SBU, we have successfully generated an expanded microporous NbO-type MOF-505 analogue (NJU-Bai12). The evacuated solid NJU-Bai12-ac shows both the highest BET surface area of 3038 m^2·g^{-1} and the largest unsaturated total H_2 adsorption capacity of 62.7 mg·g^{-1} (20 bar and 77 K) among reported MOF-505 analogues. In addition, NJU-Bai12-ac exhibits excellent CO_2 uptake capacity (23.83 and 19.85 mmol·g^{-1} at 20 bar for 273 and 298 K, respectively) and selective gas adsorption property with a CO_2/CH_4 selectivity of 5.0 and a CO_2/N_2 selectivity of 24.6 at room temperature. This work demonstrates that the ligand expansion, especially through alkyne bonds, is an effective method to boost the MOF materials' surface area and pore volume, thereby enhancing gas uptake. Work along this strategy is currently underway in our laboratory.

ASSOCIATED CONTENT

Supporting Information

Crystal data in CIF format, TGA, IR, details of calculations on gas adsorption selectivity, and isosteric heats of sorption. This material is available free of charge via the Internet at http://pubs.acs.org.

AUTHOR INFORMATION

Corresponding Author

*E-mail: zbaishu@163.com (B.Z.), bjunfeng@nju.edu.cn (J.B.).

Notes

The authors declare no competing financial interest.

ACKNOWLEDGMENTS

This work was supported by the Major State Basic Research Development Programs (Grant 2011CB808704), the NSFC (Grant 21201062, 20931004), the Science Foundation of Innovative Research Team of NSFC (Grant 20721002), and the Fundamental Research Funds for the Central Universities (Grant 1114020501).

REFERENCES

(1) Lee, J. Y.; Farha, O. K.; Roberts, J.; Scheidt, K. A.; Nguyen, S. T.; Hupp, J. T. *Chem. Soc. Rev.* **2009**, *38*, 1450.
(2) Kurmoo, M. *Chem. Soc. Rev.* **2009**, *38*, 1353.
(3) Allendorf, M. D.; Bauer, C. A.; Bhakta, R. K; Houk, R. J. T. *Chem. Soc. Rev.* **2009**, *38*, 1330.
(4) Horcajada, P.; Chalati, T.; Serre, C.; Gillet, B.; Sebrie, C.; Baati, T.; Eubank, J. F.; Heurtaux, D.; Clayette, P.; Kreuz, C.; Chang, J. S.; Hwang, Y. K.; Marsaud, V.; Bories, P. N.; Cynober, L.; Gil, S.; Férey, G.; Couvreur, P.; Gref, R. *Nat. Mater.* **2010**, *9*, 172.
(5) Rocha, J.; Carlos, L. D.; Paz, F. A. A.; Ananias, D. *Chem. Soc. Rev.* **2011**, *40*, 926.
(6) (a) Hirscher, M. *Angew. Chem., Int. Ed.* **2011**, *50*, 581. (b) Sculley, J.; Yuan, D.; Zhou, H.-C. *Energy Environ. Sci.* **2011**, *4*, 2721. (c) Han, S. S.; Mendoza-Cortes, J. L.; Goddard, W. A., III. *Chem. Soc. Rev.* **2009**, *38*, 1460.
(7) (a) Ma, S. Q.; Sun, D. F.; Simmons, J. M.; Collier, C. D.; Yuan, D. Q.; Zhou, H.-C. *J. Am. Chem. Soc.* **2008**, *130*, 1012. (b) Wu, H.; Zhou, W.; Yildirim, T. *J. Am. Chem. Soc.* **2009**, *131*, 4995. (c) Guo, Z.; Wu, H.; Srinivas, G.; Zhou, Y.; Xiang, S.; Chen, Z.; Yang, Y.; Zhou, W.; O'Keeffe, M.; Chen, B. *Angew. Chem., Int. Ed.* **2011**, *50*, 3178.
(8) (a) Ferey, G.; Serre, C.; Devic, T.; Maurin, G.; Jobic, H.; Llewellyn, P. L.; Weireld, G. D.; Vimont, A.; Daturi, M.; Chang, J.-S. *Chem. Soc. Rev.* **2011**, *40*, 550. (b) D'Alessandro, D. M.; Smit, B.;

Long, J. R. *Angew. Chem., Int. Ed.* **2010**, *49*, 6058. (c) Li, J.-R.; Ma, Y.; Mccarthy, M. C.; Sculley, J.; Yu, J.; Jeong, H.-K.; Balbuena, P. B.; Zhou, H.-C. *Coord. Chem. Rev.* **2011**, *255*, 1791.
(9) (a) Farha, O. K.; Yazaydin, A. O.; Eryazici, I.; Malliakas, C. D.; Hauser, B. G.; Kanatzidis, M. G.; Nguyen, S. T.; Snurr, R. Q.; Hupp, J. T. *Nat. Chem.* **2010**, *2*, 944. (b) Furukawa, H.; Ko, N.; Go, Y. B.; Aratani, N.; Choi, S. B.; Choi, E.; Yazaydin, A. O.; Snurr, R. Q.; O'Keeffe, M.; Kim, J.; Yaghi, O. M. *Science* **2010**, *329*, 424.
(10) (a) Eddaoudi, M.; Kim, J.; Rosi, N.; Vodak, D.; Wachter, J.; O'Keeffe, M.; Yaghi, O. M. *Science* **2002**, *295*, 469. (b) Chen, B.; Ma, S.; Zapata, F.; Lobkovsky, E. B.; Yang, J. *Inorg. Chem.* **2006**, *45*, 5718. (c) Chen, B.; Ma, S.; Zapata, F.; Fronczek, F. R.; Lobkovsky, E. B.; Zhou, H.-C. *Inorg. Chem.* **2007**, *46*, 1233.
(11) (a) Chae, H. K.; Siberio-Perez, D. Y.; Kim, J.; Go, Y. B.; Eddaoudi, M.; Matzger, A. J.; O'Keeffe, M.; Yaghi, O. M. *Nature* **2004**, *427*, 523. (b) Ferey, G.; Mellot-Draznieks, C.; Serre, C.; Millange, F.; Dutour, J.; Surble, S.; Margiolaki, I. *Science* **2005**, *309*, 2040.
(12) (a) Pan, L.; Sander, M. B.; Huang, X.; Li, J.; Smith, M. R., Jr.; Bittner, E. W.; Bockrath, B. C.; Johnson, J. K. *J. Am. Chem. Soc.* **2004**, *126*, 1308. (b) Kesanli, B.; Cui, Y.; Smith, M. R.; Bittner, E. W.; Bockrath, B. C.; Lin, W. *Angew. Chem., Int. Ed.* **2005**, *44*, 72.
(13) (a) Chen, B. L.; Ockwig, N. W.; Millward, A. R.; Contreras, D. S.; Yaghi, O. M. *Angew. Chem., Int. Ed.* **2005**, *44*, 4745. (b) Ma, S.; Zhou, H.-C. *J. Am. Chem. Soc.* **2006**, *128*, 11734. (c) Chen, B.; Xiang, S.; Qian, G. *Acc. Chem. Res.* **2010**, *43*, 1115. (d) Das, M. C.; Xiang, S.; Zhang, Z.; Chen, B. *Angew. Chem., Int. Ed.* **2011**, *50*, 10510.
(14) (a) Kitagawa, S.; Kitaura, R.; Noro, S.-I. *Angew. Chem., Int. Ed.* **2004**, *43*, 2334. (b) Wang, X.-S.; Ma, S.; Sun, D.; Parkin, S.; Zhou, H.-C. *J. Am. Chem. Soc.* **2006**, *128*, 16474. (c) Bradshaw, D.; Claridge, J. B.; Cussen, E. J.; Prior, T. J.; Rosseinsky, M. J. *Acc. Chem. Res.* **2005**, *38*, 273.
(15) (a) Zhao, D.; Yuan, D. Q.; Zhou, H. C. *Energy Environ. Sci.* **2008**, *1*, 222. (b) Frost, H.; Düren, T.; Snurr, R. Q. *J. Phys. Chem. B* **2006**, *110*, 9565.
(16) (a) Lin, X.; Jia, J.; Zhao, X.; Thomas, K. M.; Blake, A. J.; Walker, G. S.; Champness, N. R.; Hubberstey, P.; Schröder, M. *Angew. Chem., Int. Ed.* **2006**, *45*, 7358. (b) Dincă, M.; Dailly, A.; Tsay, C.; Long, J. R. *Inorg. Chem.* **2008**, *47*, 11−13.
(17) Farha, O. K.; Wilmer, C. E.; Eryazici, I.; Hauser, B. G.; Parilla, P. A.; O'Neill, K.; Sarjeant, A. A.; Nguyen, S. T.; Snurr, R. Q.; Hupp, J. T. *J. Am. Chem. Soc.* **2012**, *134*, 9860.
(18) Farha, O. K.; Eryazici, I.; Jeong, N. C.; Hauser, B. G.; Wilmer, C. E.; Sarjeant, A. A.; Snurr, R. Q.; Nguyen, S. T.; Yazaydın, A. Ö.; Hupp, J. T. *J. Am. Chem. Soc.* **2012**, *134*, 15016−15021.
(19) (a) Luo, J.; Xu, H.; Liu, Y.; Zhao, Y.; Daemen, L. L.; Brown, C.; Timofeeva, T. V.; Ma, S.; Zhou, H.-C. *J. Am. Chem. Soc.* **2008**, *130*, 9626. (b) Xue, M.; Zhu, G.; Li, Y.; Zhao, X.; Jin, Z.; Kang, E.; Qiu, S.-L. *Cryst. Growth Des.* **2008**, *8*, 2478. (c) Lee, Y. G.; Moon, H. R.; Cheon, Y. E.; Suh, M. P. *Angew. Chem., Int. Ed.* **2008**, *47*, 7741. (d) Wang, X. S.; Ma, S.; Rauch, K.; Forster, P. M.; Yuan, D.; Eckert, J.; Lopez, J. L.; Murphy, B. J.; Parise, J. B.; Meijere, A.; Zhou, H.-C. *Angew. Chem., Int. Ed.* **2008**, *47*, 7263. (e) Wang, X. S.; Ma, S.; Rauch, K.; Simmons, J. M.; Yuan, D.; Wang, X.; Yildirim, T.; Cole, W. C.; Lopez, J. L.; Meijere, A.; Zhou, H.-C. *Chem. Mater.* **2008**, *20*, 3145. (f) Lin, X.; Telepeni, I.; Blake, A. J.; Dailly, A.; Brown, C.; Simmons, J.; Zoppi, M.; Walker, G. S.; Thomas, K. M.; Mays, T. J.; Hubberstey, P.; Champness, N. R.; Schröder, M. *J. Am. Chem. Soc.* **2009**, *131*, 2159. (g) Sun, D.; Ma, S. J.; Simmons, M.; Li, J.-R.; Yuan, D.; Zhou, H.-C. *Chem. Commun.* **2010**, *46*, 1329. (h) Zhao, D.; Yuan, D.; Yakovenko, A.; Zhou, H.-C. *Chem. Commun.* **2010**, *46*, 4196. (i) Prasad, T. K.; Hong, D. H.; Suh, M. P. *Chem.—Eur. J.* **2010**, *16*, 14043.
(20) (a) Zheng, B.; Dong, H.; Bai, J.; Li, Y. Z.; Li, S. H.; Scheer, M. *J. Am. Chem. Soc.* **2008**, *130*, 7778. (b) Hu, Y.; Xiang, S.; Zhang, W.; Zhang, Z.; Wang, L.; Bai, J.; Chen, B. *Chem. Commun.* **2009**, 7551. (c) Zheng, B.; Bai, J.; Duan, J.; Wojtas, L.; Zaworotko, M. J. *J. Am. Chem. Soc.* **2011**, *133*, 748. (d) Duan, J.; Bai, J.; Zheng, B.; Li, Y.; Ren, W. *Chem. Commun.* **2011**, *47*, 2556. (e) Duan, J.; Yang, Z.; Bai, J.; Zheng, B.; Li, Y.; Li, S. *Chem. Commun.* **2012**, 3058. (f) Zheng, B.; Yang, Z.; Bai, J.; Li, Y.; Li, S. *Chem. Commun.* **2012**, 7025.
(21) Zhou, H.; Dang, H.; Yi, J.-H.; Nanci, A.; Rochefort, A.; Wuest, J. D. *J. Am. Chem. Soc.* **2007**, *129*, 13774.
(22) Sheldrick, G. M. *Acta Crystallogr., Sect. A* **2008**, *64*, 112.
(23) Spek, A. L. *J. Appl. Crystallogr.* **2003**, *36*, 7.
(24) (a) Kaye, S. S.; Dailly, A.; Yaghi, O. M.; Long, J. R. *J. Am. Chem. Soc.* **2007**, *129*, 14176. (b) Furukawa, H.; Miller, M. A; Yaghi, O. M. *J. Mater. Chem.* **2007**, *17*, 3197.
(25) Rowsell, J. L. C.; Yaghi, O. M. *J. Am. Chem. Soc.* **2006**, *128*, 1304.
(26) Yan, Y.; Lin, X.; Yang, S.; Blake, A. J.; Dailly, A.; Champness, N. R.; Hubbersteya, P.; Schröder, M. *Chem. Commun.* **2009**, 1025.
(27) *Materials Studio*, version 4.1; Accelrys: San Diego, CA, 2006.
(28) Hong, S.; Oh, M.; Park, M.; Yoon, J. W.; Chang, J.-S.; Lah, M. S. *Chem. Commun.* **2009**, 5397.
(29) DOE Targets for On-Board Hydrogen Storage Systems for Light-Duty Vehicles, available at http://www1.eere.energy.gov/hydrogenandfuelcells/storage/ current_technology.html.
(30) (a) Collins, D. J.; Zhou, H.-C. *J. Mater. Chem.* **2007**, *17*, 3154. (b) Dincă, M.; Dailly, A.; Liu, Y.; Brown, C. M.; Neumann, D. A.; Long, J. R. *J. Am. Chem. Soc.* **2006**, *128*, 16876. (c) Rowsell, J. L. C.; Yaghi, O. M. *Angew. Chem., Int. Ed.* **2005**, *44*, 4670. (d) Latroche, M.; Surblé, S.; Serre, C.; Mellot-Draznieks, C.; Llewellyn, P. L.; Lee, J.-H.; Chang, J.-S.; Jhung, S. H.; Férey, G. *Angew. Chem., Int. Ed.* **2006**, *45*, 8227. (e) Suh, M. P.; Park, H. J.; Prasad, T. K.; Lim, D.-W. *Chem. Rev.* **2012**, *112*, 782.
(31) (a) Yan, Y.; Telepeni, I.; Yang, S.; Lin, X.; Kockelmann, W.; Dailly, A.; Blake, A. J.; Lewis, W.; Walker, G. S.; Allan, D. R.; Barnett, S. A.; Champness, N. R.; Schröder, M. *J. Am. Chem. Soc.* **2010**, *132*, 4092. (b) Yan, Y.; Yang, S.; Blake, A. J.; Lewis, W.; Poirier, E.; Barnett, S. A.; Champnessa, N. R.; Schröder, M. *Chem. Commun.* **2011**, *47*, 9995.
(32) Figueroa, J. D.; Fout, T.; Plasynski, S.; McIlvried, H.; Srivastava, R. D. *Int. J. Greenhouse Gas Control* **2008**, *2*, 9.
(33) (a) Hao, G.-P.; Li, W.-C.; Lu, A.-H. *J. Mater. Chem.* **2011**, *21*, 6447. (b) Zhang, J.; Singh, R.; Welbley, P. A. *Microporous Mesporous Mater.* **2008**, *111*, 478. (c) Bernal, M. P.; Coronas, J.; Menéndez, M.; Santamaria, J. *AIChE J.* **2004**, *50*, 127. (d) Cavenati, S.; Grande, C. A.; Rodrigues, A. E. *J. Chem. Eng. Data* **2004**, *49*, 1095. (e) Ebner, A. D.; Reynolds, S. P.; Ritter, J. A. *Ind. Eng. Chem. Res.* **2007**, *46*, 1737.
(34) (a) D'Alessandro, D. M.; Smit, B.; Long, J. R. *Angew. Chem., Int. Ed.* **2010**, *49*, 2. (b) Ma, S. Q.; Zhou, H. C. *Chem. Commun.* **2010**, *46*, 44. (c) Simmons, J. M.; Wu, H.; Zhou, W.; Yildirim, T. *Energy Environ. Sci.* **2011**, *4*, 2177.
(35) (a) Millward, A. R.; Yaghi, O. M. *J. Am. Chem. Soc.* **2005**, *127*, 17998. (b) Babarao, R.; Jiang, J. *Langmuir* **2008**, *24*, 6270. (c) Finsy, V.; Ma, L.; Alaerts, L.; De Vos, D. E.; Baron, G. V.; Denayer, J. F. M. *Microporous Mesoporous Mater.* **2009**, *120*, 221.
(36) (a) Férey, G. *Chem. Soc. Rev.* **2008**, *37*, 191. (b) Xiang, S.; He, Y.; Zhang, Z.; Wu, H.; Zhou, W.; Krishna, R.; Chen, B. *Nat. Commun.* **2012**, *3*, 954.
(37) Sumida, K.; Horike, S.; Kaye, S. S.; Herm, Z. R.; Queen, W. L.; Brown, C. M.; Grandjean, F.; Long, G. J.; Dailly, A.; Long, J. R. *Chem. Sci.* **2010**, *1*, 184.
(38) (a) An, J.; Geib, S. J.; Rosi, N. L. *J. Am. Chem. Soc.* **2010**, *132*, 38. (b) Banerjee, R.; Furukawa, H.; Britt, D.; Knobler, C.; O'Keeffe, M.; Yaghi, O. M. *J. Am. Chem. Soc.* **2009**, *131*, 3875.
(39) Saha, D.; Bao, Z. B.; Jia, F.; Deng, S. G. *Environ. Sci. Technol.* **2010**, *44*, 1820.